



**INTERNATIONAL JOURNAL OF ENGINEERING SCIENCES & RESEARCH  
TECHNOLOGY**

**STUDYING THE DIELECTRIC PROPERTIES, MICROSTRUCTURE AND  
MORPHOLOGY OF DOPED NANOFERRITE COMPOSITE**

**Prof. Dr. Fadhil A. Chyad, Asst. Prof. Dr. Mohammed S. Hamza and Asst. Lecturer Zainab I. Dhary**  
Dept. of Materials Engineering, University of Technology, Baghdad - IRAQ

**ABSTRACT**

Mixed ferrite having the general formula  $(Li_{0.5}Fe_{0.5}O_4)_{0.9}(Co_4Fe_2O_4)_{0.1}$  doped with different percentage of  $Y_2O_3$  were prepared using autocombustion method. X-ray diffraction (XRD) reveals the polycrystalline nature of the samples. TEM micrograph gave the evidence of preparing the nanoparticles, where the average particle size was (8-20) nm. Some moderately agglomerated particles as well as separated particles are present in the images. SEM micrographs revealed that the microstructure of the fracture surface of samples consists of detached approximately closely packed particles and also showed the formation of micro agglomerated particles with some voids. By doping with  $Y_2O_3$  the pores decreased and a dense material obtained. Dielectric properties were decreased with frequency while the highest value of dielectric constant at 1 wt. % of  $Y_2O_3$ .

**Keywords:** Nanoferrite,  $Y_2O_3$ , Dielectric constant, XRD, TEM, SEM.

**INTRODUCTION**

Spinel ferrite is an important class of electrical materials because of their high resistivity and low loss behavior. Ferrite are performed in the field of electronics and telecommunication industry because of their navel electric properties which make them useful in radiofrequency circuit, high quality factor, rod antennas, transformer core, and read / write heads for high density, digital tapes (1,2)

Polycrystalline ferrites are very good dielectric materials where their properties depend on several factors, such as method of preparation, sintering conditions, chemical composition and crystalline size (3)

Lithium ferrite is an unusual and, in the same respect, a remarkable material. Where, several research programs have been undertaken to study its fundamental properties and to develop high-power microwave materials from it. Among the distinctive properties of lithium ferrite are the following:

1- The lithium ion is monovalent; i.e., in order to preserve charge balance,  $Li^+$  enters the lattice in

<http://www.ijesrt.com>

combination with  $Fe^{3+}$  ion. The compound may be thought of as  $(Li_{2.5}Fe_{0.5})Fe_2O_4$ . lithium ferrite can be prepared with low value of  $\Delta H$ .

2- An ionic ordering can be established in lithium ferrite. Lithium enters the spinel lattice on the octahedral sites (i.e., the spinel is inverted).

Above  $750^\circ C$ , the arrangement of Fe and Li ions on the octahedral site is disordered. If the material is suddenly cooled (quenched) from this temperature, the disorder is preserved. However, slow cooling causes the ions to distribute themselves in a regular pattern:  $3Fe^{3+}$  followed by one ( $Li^+$ ) in rows along the [110] direction, this crystal, therefore, provides a way to determine the effect of volume disorder, particularly on line width [4].

Rare earth ions have unpaired 4f electrons that have a role to originate magnetic anisotropy due to their orbital shape, where the magneto-crystalline

anisotropy in ferrites is related to 4f-3d coupling between the transition metal and rare earth ions, thereby doping rare-earth ions into spinel Li-Ni ferrite can improve their electrical and magnetic properties [5].

Reddy (1988), studied the mixed ferrite  $(Li_{0.5}Fe_{0.5})_{1-x}Ni_xFe_2O_4$  and claimed to be the first study of this kind of ferrites. He measured the electrical conductivity and thermoelectric power as a function of the composition and temperature. Charge carriers mobility, dielectric constant, and loss tangent have been studied at low frequencies [6].

Jacintho et al. (2009) investigated the structural investigation of  $MFe_2O_4$  (M) Fe, (Co) magnetic fluids. Ferrites of the type  $MIFe_2O_4$  (M) Fe and Co) were prepared by the traditional co-precipitation method. These ferrites were modified by the adsorption of fatty acids derived from soybean and castor oil and were then dispersed in cyclohexane, providing very stable magnetic fluids, readily usable in nonpolar media. XRD and TEM analysis showed that the magnetic nanoparticles (nonmodified and modified) present with diameters in the range of (10-15) nm [7].

Mazen and Elmosalami (2011), studied the structural and elastic properties of a spinel ferrite like Li-Ni ferrite which has the chemical formula  $Li_{0.5-0.5x}Ni_xFe_{2.5-0.5x}O_4$  ( $0.0 \leq x \leq 1.0$ ) have been prepared by the ceramic method. The spinel structure in homogenous state was realized by X-ray diffraction analysis. The lattice parameter has been determined for each composition and found to be nearly constant over the whole range of Niconcentration ( $0.83 \text{ nm} \pm 0.01$ ). The analysis of IR

spectra indicates the presence of splitting in the absorption band due to the presence of small amounts of  $Fe^{2+}$  ions in the ferrite system. Young's modulus (E), rigidity modulus (G), has been determined. The variation of elastic moduli with composition has been interpreted in terms of binding forces between the atoms of spinal lattice [8].

Arana et al. (2012) studied the Li-substituted Mn-Zn ferrite structural and magnetic properties after different thermal treatments. Spinel ferrites which has the chemical formula  $Zn_{0.6}Mn_{0.4}Fe_2O_4$  and  $Li_{0.2}Zn_{0.2}Mn_{0.4}Fe_{2.5}O_4$  were prepared by the self-combustion sol-gel method. Incorporating Li to the crystalline lattice increased the saturation magnetization and promoted a decrease in the secondary phase's segregation. This result was explained assuming that the Li incorporation produced a cationic redistribution in the spinel structure [9].

Mohapatra et al. (2013), investigated the surface controlled synthesis of  $MFe_2O_4$  (M = Mn, Fe, Co, Ni and Zn) nanoparticles and their magnetic characteristics. The particle sizes between (2–9) nm were tuned by simple manipulation of the amine to precursor molar ratio while the larger sizes (12–16 nm) were attained by the seed-mediated growth. The synthesized nanoparticles are magnetic and showed cubic-spinel structure as characterized by XRD and Raman spectroscopy [10].

Chyad et al have studied the dielectric properties of mixed ferrite  $(Li_{0.5}Fe_{0.5}O_4)_{1-x}(Co_4Fe_2O_4)_x$ . Crystalline structure by XRD and dielectric properties with TEM micrographs have been presented. TEM micrographs show a nano particales

in the range(8-20)nm. Dielectric properties have been decreased with frequency and Cobalt content [11].

Agami et. al. (2014), investigated the structural, IR, and magnetic studies of annealed Li-ferrite nanoparticles nano-particles of spinel Li-ferrite,  $\text{Li}_{0.5}\text{Fe}_{2.5}\text{O}_4$ , were prepared by sol-gel autocombustion technique and annealed at different temperatures ( $T_a = 673, 873, \text{ and } 1073 \text{ K}$ ). The saturation magnetization ( $M_s$ ) increased, and the surface area decreased by increasing the crystallite size, while Curie temperature ( $T_C$ ) remained almost constant [12].

Nlebedim and Jiles (2014), studied the effect of titanium substitution on the structural and magnetic properties of cobalt–ferrite. Spinel crystal structure in ferrites presents various degrees of freedom in altering their magnetic and related properties to specific ferrite has been found to result in a non-linear variation in lattice parameter [13]

Chyad et al have prepared a mixed ferrite  $(\text{Li}_{2.5}\text{Fe}_{0.5}\text{O}_4)_{0.9}(\text{Co}_4\text{Fe}_2\text{O}_4)_{0.1}$  with different percentages of  $\text{Y}_2\text{O}_3$ . Physical properties (density, porosity and water absorption) were affected by the doping, where the density is increased while the porosity has drastically decreasing and has a correlation effect on the mechanical properties (splitting tensile strength and Vickers microhardness). The fracture strength at 1wt%  $\text{Y}_2\text{O}_3$  has doubled value of the undoped sample[14]

The aim of this work is to prepare nanomixed – ferrites doping with different percentages of  $\text{Y}_2\text{O}_3$  and studying their structural, morphology and dielectric properties of the system.

## MATERIALS AND METHODS

### *Starting materials*

The raw materials used to prepare Lithium – Cobalt ferrite by sol – gel method were cobalt nitrate ( England ) , lithium nitrate ( England ) , iron nitrate ( Spain ) , citric acid ( Germany ) as fuel , ammonium hydroxide ( Spain ) , glucose (USA) polyvinyl alcohol (USA) and  $\text{Y}_2\text{O}_3$  ( China ) .

### *Preparation of Nano-Ferrite by Co-precipitation:*

1. Hydrated cobalt nitrate is dissolved in 50/50 % distilled water – ethanol ratio with 0.5 M.
2. Hydrated lithium nitrate is dissolved in 50/50 % distilled water – ethanol ratio with 0.5 M.
3. Hydrated iron nitrate is dissolved in 50/50 % distilled water – ethanol ratio with 0.5 M.
4. The cobalt solution is mixed with iron solution, where the ratio of cobalt solution to iron solution was selected according to a definite chemical stoichiometric ratio as (Fe: Co=2:1) by using magnetic stirrer.
5. The lithium solution is mixed with iron solution, where the ratio of lithium solution to iron solution was selected according to a definite chemical stoichiometric ratio as (Fe: Li =5:1) by using magnetic stirrer.
6. The two solutions are mixed by using magnetic stirrer.
7. Addition of the resulting cobalt ferrite with different weight percentage (2, 5, 10, 15 and 20 wt. %) to lithium ferrite.
8. Addition of surfactant material (glucose).
9. Addition of ammonium hydroxide drops to the mixed solution until the gel bed was formed.

- 10. PH of the solution was measured, where the gel formation begins at PH 6.5.
- 11. Addition of citric acid that leads to hear notifying the combustion which helps in reducing the particle size of produced gel.
- 12. Filtrate the solution with filter papers to get out the gel.

The sintering processes of the compact samples were carried out in air atmosphere. The sintering temperature used was 1200 °C for two hours, with a heating rate and cooling rate of 10°C /min. Then, the dimensions and masses of sintered samples were measured to determine the densities.

*Characterization Techniques*

The composite powders of (lithium ferrite - cobalt ferrite) from the composition  $(Li_{0.5}Fe_{2.5}O_4)_{0.9} (CoFe_2O_4)_{0.1}$  with different percentages of  $Y_2O_3$  were analyzed by X-ray diffraction operated at 35 KV, 40 mA, using Cu-K $\alpha$  radiation, as shown in figure (3.4). Also, X-ray diffraction was used to identify the crystal structure for the compact samples after the sintering process. The diffracted X-ray intensity was recorded versus the diffraction angle (2 $\theta$ ).

*Scanning Electron Microscope (SEM)*

Microstructures of sintered compacts were observed in a scanning electron microscope. The fracture surface of selected specimens was examined.

The specimen stub was inserted on the specimen holder and was adjusted to the proper height using the specimen height gauge.

Transmission Electron Microscope:

Investigation of the morphology and the homogeneity of the composite powders of lithium ferrite-cobalt ferrite  $(Li_{0.5}Fe_{2.5}O_4)_{0.9} (CoFe_2O_4)_{0.1}$  after the calcination step was carried out by using TEM operating at 600 KV.

*Dielectric properties:*

The electrical behavior is usually strongly dependent upon temperature and composition for example; a small change in the composition may transform an insulating ceramic in to a semiconductor. Ceramic materials will be considered throughout in terms of insulators and type of bonds involved may be ionic or covalent.

Dielectric constant or permittivity ( $\epsilon$ ) is the ratio of the amount of energy stored in the dielectric to that stored by air occupying the same volume. It is a measure of electric storage ability, or capacitance.

The capacitance of insulated portion depends on the geometrical dimensions and the shape of the electrodes, and on the material of the dielectric.

For capacitor of any arbitrary shape and dimensions with vacuum in the space between the electrodes (vacuum capacitor), its capacitance ( $C_o$ ) is given:

$$C_o = \epsilon_o \frac{A}{d} \dots\dots\dots(1)$$

Where:

$\epsilon_o = 8.85 \cdot 10^{-12}$  (F/M) for vacuum.

A= cross-sectional area of the insulator.

d= distance between the capacitor plates.

When an insulator is placed between the electrodes, then the capacitance becomes:

$$C = \epsilon \frac{A}{d} \dots\dots\dots(2)$$

Where the  $\epsilon$  is the permittivity of the insulator.

The relative permittivity is:

$$\epsilon_r = \frac{\epsilon}{\epsilon_0} \dots\dots\dots (3)$$

$$C = \frac{\epsilon_0 \epsilon_r A}{d}$$

$$\text{Or } \epsilon_r = \frac{Cd}{\epsilon_0 A} \dots\dots\dots (4)$$

Where the imaginary part of dielectric constant  $\epsilon''$  which is called dielectric loss factor can be calculated using the following relation:

$$\epsilon'' = \epsilon \tan \delta \dots\dots\dots (5)$$

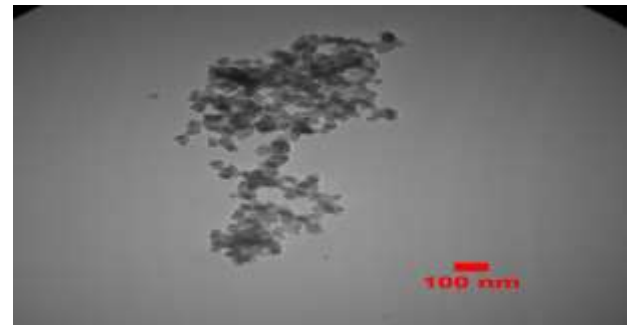
Where  $\tan \delta$  is the loss tangent [15].

**RESULTS AND DISCUSSION**

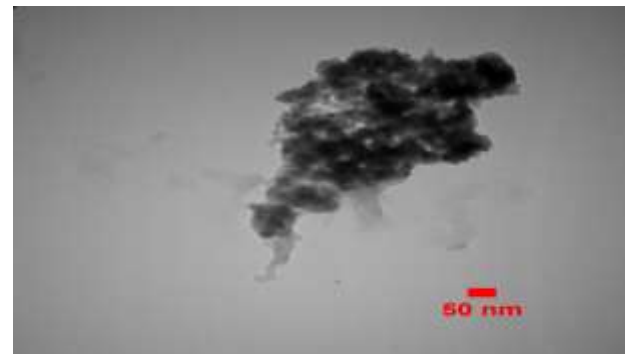
*Transmission Electron Microscopic results:*

Fig. (1) shows the (TEM) bright field micrographs for lithium-ferrite mixed with different percentages of cobalt-ferrite at 800°C for two hours. Using 7% surfactant agent (glucose) prevents the agglomeration of powder to such a percent and also prevents the grain growth of the materials [16]. This figure illustrates the size and shape of the ferrite particles extracted from the powder reduced at 800°C for two hours. This figure shows the ferrite particle size ranging from (8-20) nm. All particles resulting from the route of powder preparation have been showed regular and nearly round shape appearance and all particles were in good contact to each other. These finer particles sizes will improve the mechanical properties as will be seen later. Some appreciable formation of heavy agglomerated powders was present and this was attributed to the large surface area of these nanoparticles. The agglomeration refers to the adhesion of the particles to each other because of Vander Walls force of attraction which are significantly higher in nanoparticles.

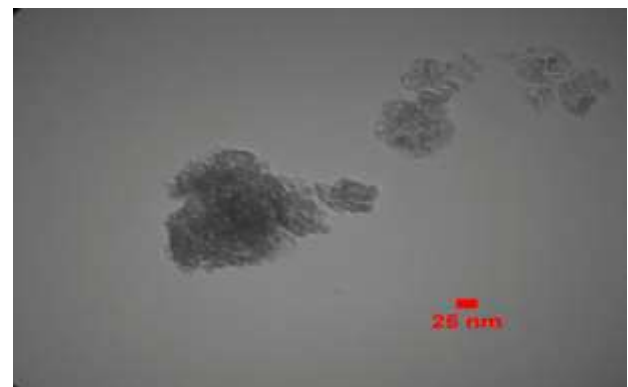
These images manifest the distribution of ferrite nanoparticles, which sometimes seem to by symmetric (Gaussian) about less than 10 nm in average size. Some moderately agglomerated particles as well as separated particles are present in the images.



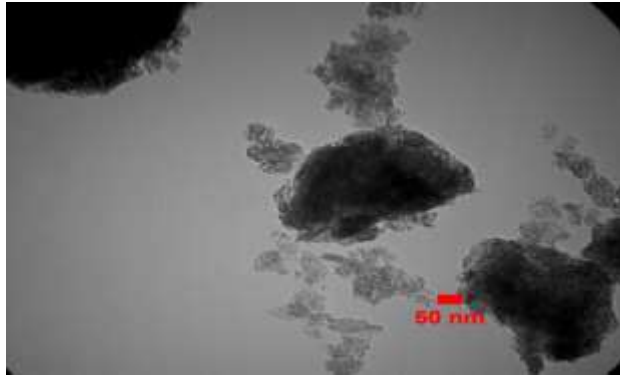
a



b



c



d

**Figure (1): TEM images for prepared nano ferrite powder after calcination at 800°C for 1 hr.**

#### X-ray Diffraction for Nano-Ferrite powders:

Fig. (2) shows the powder X-ray diffraction patterns of the synthesized powders of lithium-ferrite and cobalt-ferrite alone and the mixing between the two ferrites after calcination at 800°C for 1hr. The diffraction peaks of all the samples assigned to cubic fluorite are consistent with the JCPDS (Joint committee on powder diffraction standard) database for phase identification of lithium ferrite and cobalt ferrite. The peaks are appreciably sharpened which indicate higher crystallinity. Adding the percentages of cobalt ferrite has shifted the peaks for higher angles diffraction.

Figs. (3 -5) represent the XRD pattern of the ferrite system dope with 0.5 and 2 wt. %  $Y_2O_3$  respectively. All the  $Y_2O_3$  substituted the ferrite system  $[(Li_{0.5}Fe_{2.5}O_4)_{1-x}(CoFe_2O_4)_x]$  at the various compositions show the crystalline cubic spinel structure. The sharp peaks represent that all ferrites are crystalline nature of single phase, where all the peaks have shifted. The calculated lattice parameter is seen to increase with increasing  $Y_2O_3$  content. A similar behavior of lattice parameter with doping

concentration was observed by investigators in various ferrite systems [17-18]. The variation in lattice parameter can be explained on the basis of the ionic radius of Y ion (0.106) nm which is higher than of  $Li^+$  and  $Co^{+2}$ .

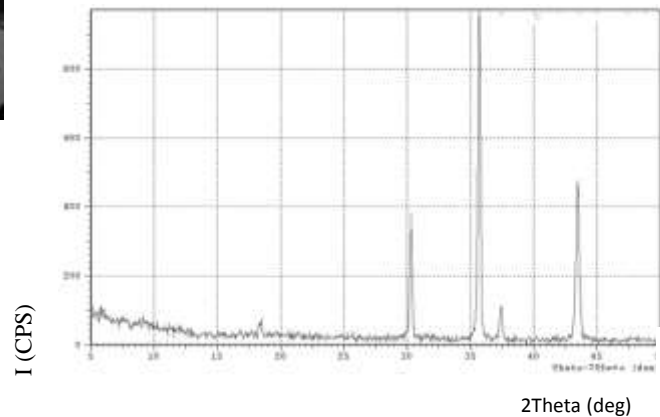


**Figure (2): XRD pattern of lithium-ferrite doped with 10% cobalt-ferrite after calcination at 800 °C.**

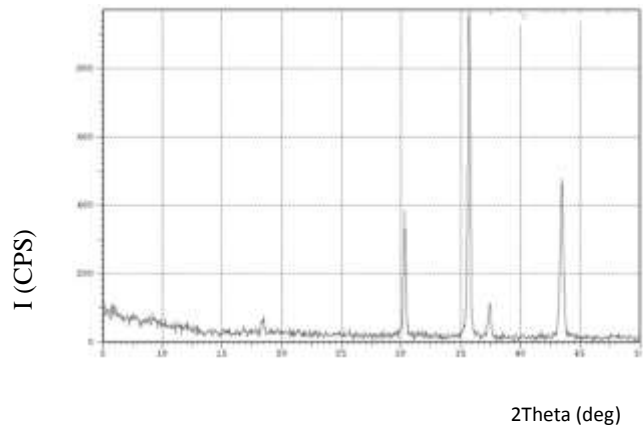


**Figure (3): XRD pattern of the ferrite system doped with 0.5 wt. %  $Y_2O_3$ .**

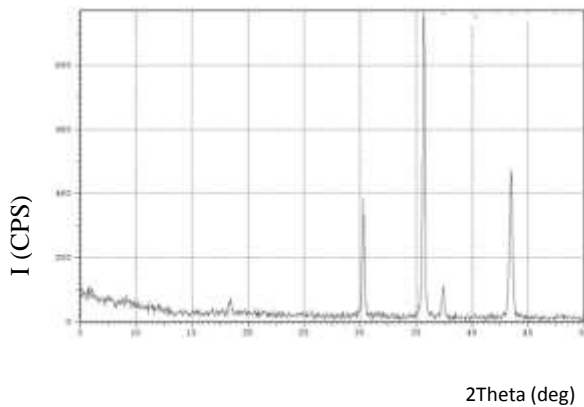


**Figure (4): XRD pattern of the ferrite system doped with 2 wt. %  $Y_2O_3$**

#### SEM of Doped Nano-Ferrites:

SEM imaging was conducting to observe the shape and morphology of samples. The SEM micrographs were taken from the fresh fracture surface of a ferrite body compacted and sintered at  $1200^{\circ}C$  from the composition  $[(Li_{0.5}Fe_{2.5}O_4)_{1-x}(CoFe_2O_4)_x]_{1-y}(Y_2O_3)_y$  obtained with the classical ceramic technology presented. These micrographs are shown in figs. (5-9). It is clear that the fracture surface is an intergranular fracture (equiaxial), and the microstructure displays an irregular (non- equiaxial) fine grain microstructure with average grain size that are slightly larger than the ferrite powders particle size. It is evident from the micrographs that the microstructure of the surface consists of detached, approximately closely-packed particles. Also, these images show the formation of micro agglomeration particles and some voids, where pores are located at the junctions of agglomerates. The black and dark regions correspond to the ferrites particles and pores respectively, while the lighter areas are for  $Y_2O_3$  phase. Furthermore, it is clear that by increasing  $Y_2O_3$ , the porosity decreased and denser materials

obtained. The crack propagation occurs near the pores in the microstructure, where the pores act as stress concentration resulting in easy crack propagation path. It is also clear that some of the grains have grown when the sintering at  $1200^{\circ}C$  in the preferred orientation. The fracture nature of the prepared nanoferrite from lithium ferrite-10% cobalt ferrite - Yttrium Oxide seems to be brittle which is clear from the fracture samples after the indirect tensile test (Brazilian test).

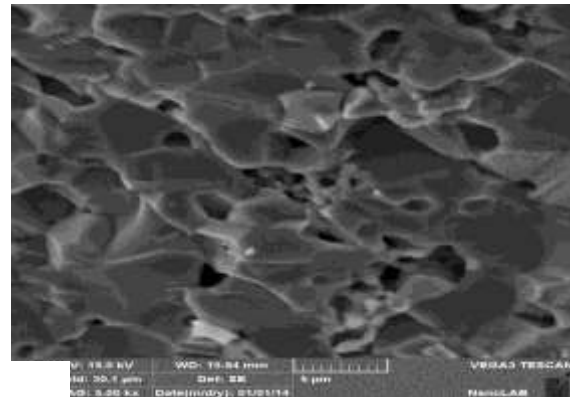


**Figure (5): SEM image of fracture surface for 0.5%  $Y_2O_3$  additives.**

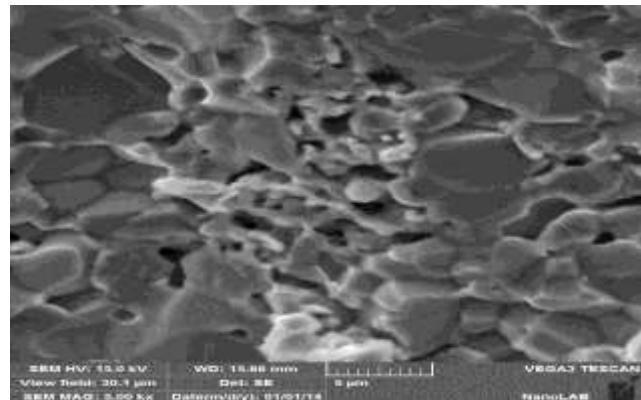


**Figure (6): SEM image of fracture surface for 1%  $Y_2O_3$  additives.**

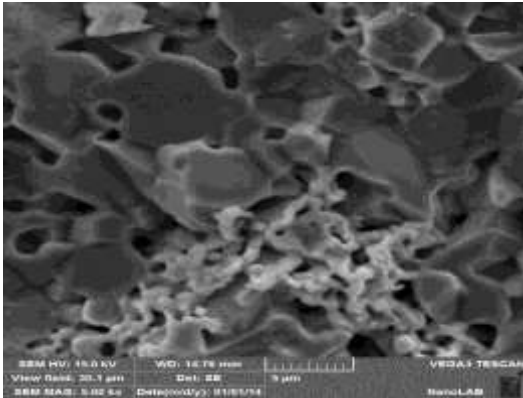


Figure (7): SEM image of fracture surface for 2%  $Y_2O_3$  additives.

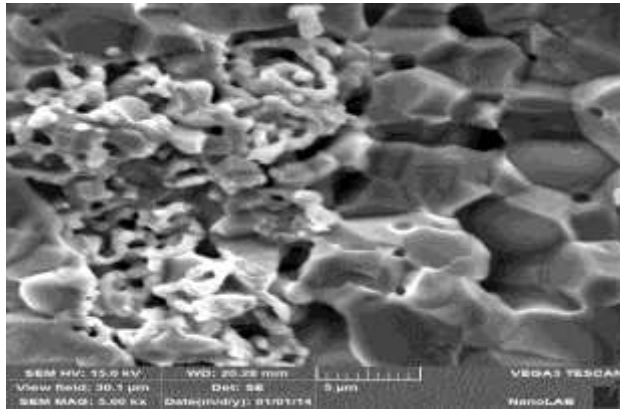


Figure (8): SEM image of fracture surface for 4%  $Y_2O_3$  additives.

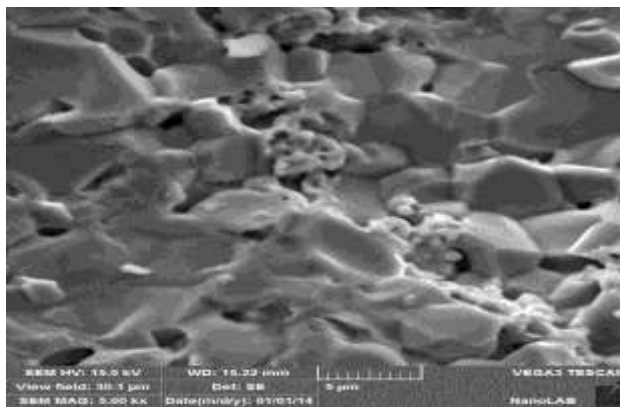


Figure (9): SEM image of fracture surface for 6%  $Y_2O_3$  additives.

### *Dielectric Properties of Doped Nano-Ferrite:*

#### *Dielectric constant:*

Figure (10) displays the variation of dielectric constant as a function of frequency at room temperature. Generally, the dielectric constant decreases with increasing frequency. The decrease of dielectric constant with  $Y^{+3}$  ion substitution may be due to the basis of the mechanism of polarization process in ferrites, which is similar to that of the conduction process. This behavior indicates the usual dispersion which can be due to the Maxwell-Wegner type interfacial polarization in accordance with Koop's phenomenological theory [19]. According to this theory, the conductivity of grain boundary contributes more to the dielectric value at lower frequencies. In this model, the dielectric structure is assumed to consist of well-conducting grains which are separated by poorly conducting grain boundaries.

For ferrite, the dielectric constant is directly proportional to the square root of conductivity [20]. The strains have a higher value of conductivity and dielectric constant, while the strain boundaries have lower values of these. Therefore, the dielectric constant is higher at lower frequencies and decreases with frequency.

In the present case, it is observed that the dielectric constant continuous to decrease with the increase of  $Y^{+3}$  ion concentration in ferrite system. This may be due to increase of resistivity of the ferrite with the substitution of  $Y^{+3}$  concentrations, as the dielectric behavior is directly proportional to the conductivity. A similar variation of the dielectric



constant with frequency was observed earlier for substitution lithium- ferrite [21]. As shown from the figure (11) that 1wt.%  $Y_2O_3$  has the highest dielectric constant and then decrease with high percentages.

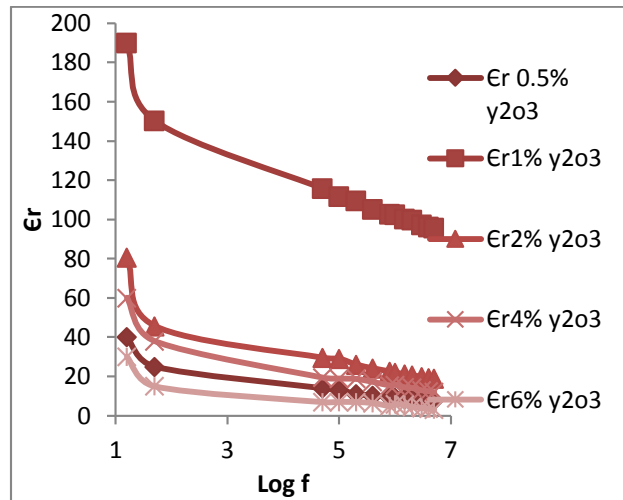


Figure (10): The relation between dielectric constant and frequency of ferrite system different percentages of  $Y_2O_3$ .

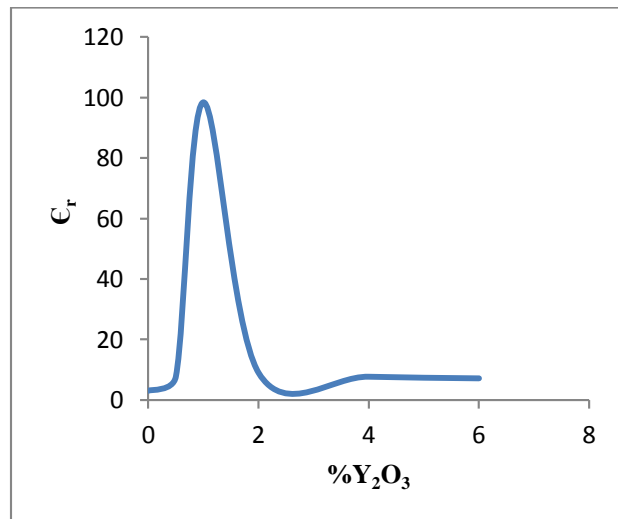


Figure (11): The effect of  $Y_2O_3$  content on the dielectric constant of ferrite system at 1MHz.

Loss tangent ( $\tan \delta$ ):

The variation of dielectric loss tangent ( $\tan \delta$ ) with frequency of ferrite system at different percentages of  $Y_2O_3$  is shown in figure (12). The abnormal behavior was observed for the samples at low frequency. The Loss tangent decreased continuously with increasing frequency and nearly attained a constant value at higher frequencies, where domain wall motion is inhibited and magnetization is changed by rotation, and hence losses are found to be lower [22]. Similar results have been reported by Kumar et. al. [23] in case of lithium ferrite and Ahmed et. al. [24] in case of nickel ferrite. Figure (13) shows the highest value of loss tangent with 1wt.%  $Y_2O_3$  and then decreased with high percentages.

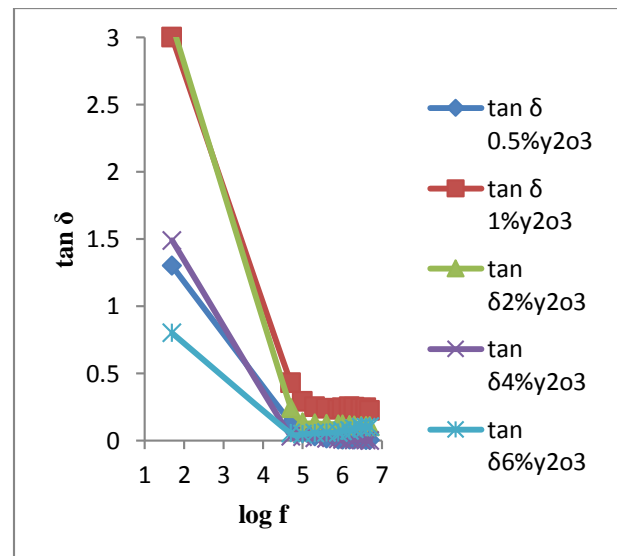


Figure (12): The effect of frequency on the loss tangent of ferrite system at different percentages of  $Y_2O_3$ .

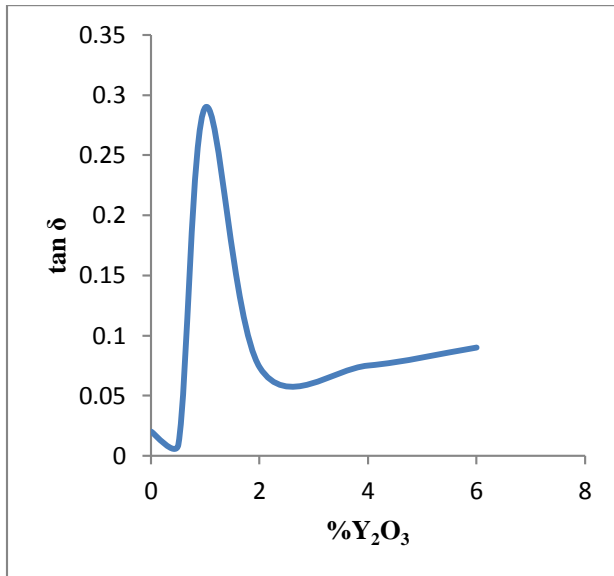


Figure (13): The effect of  $Y_2O_3$  content on the ( $\tan \delta$ ) of ferrite system at 1MHz.

Dielectric Loss Factor ( $\epsilon''$ ):

The dielectric loss factor is considered to be the most important part of the total loss in ferrite [25]. Variation of loss factor with frequency is shown in figure (14). The pattern of variation is similar to that of dielectric constant. The decrease in imaginary part of dielectric constant is pronounced more in comparison to real dielectric constant. The low dielectric values make these ferrites useful in higher frequency applications. Figure (15) shows that the highest value of dielectric loss factor are 1wt.%  $Y_2O_3$  and then decreased as the percentage increased.

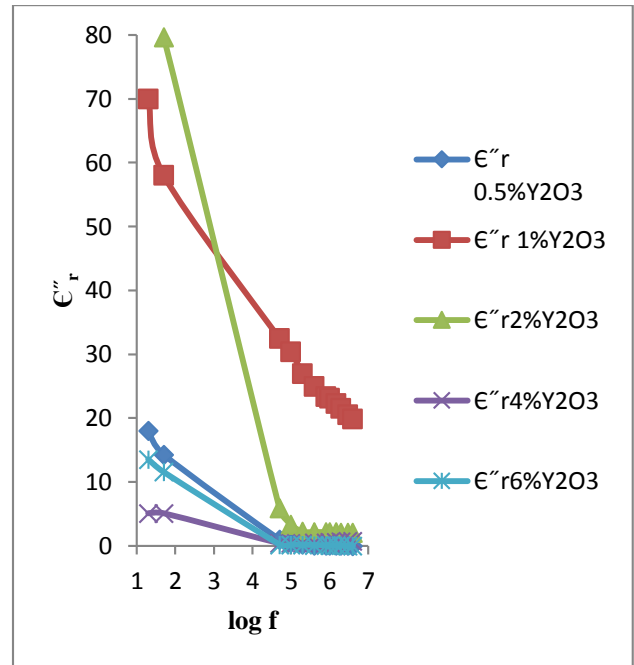


Figure (14): The variation of loss factor with frequency of ferrite system at different percentages of  $Y_2O_3$ .

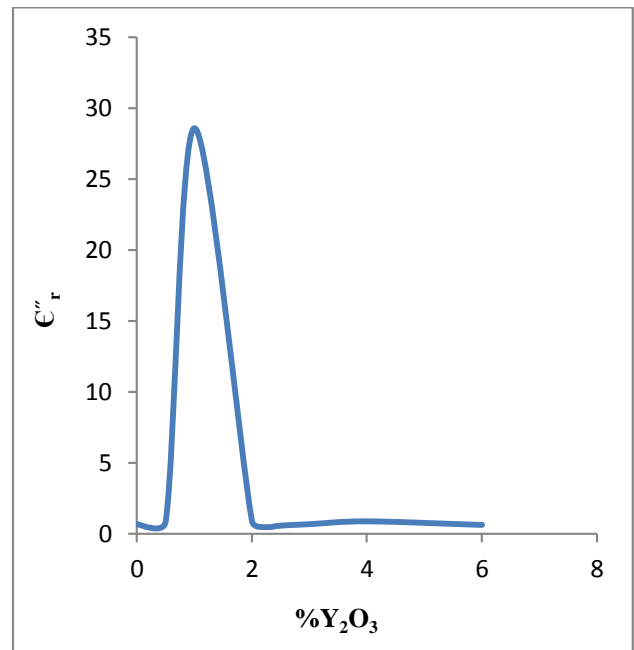


Figure (15): The effect of  $Y_2O_3$  content on loss factor of ferrite system at 1MHz.

## CONCLUSION

To summarize the main ideas obtained, the following conclusions can be drawn from this work:

- 1- Mixed ferrites (lithium ferrites-cobalt ferrite) were successfully prepared by sol-gel technique.
- 2- The microstructure of ferrite ceramic prepared by this technique consists of crystallite with clearly seen spinel cubic forms.
- 3- Structural studies proved the nanocrystalline nature of the samples.
- 4- TEM shows nanoparticles agglomeration with some separate particles in the range (8-20) nm size.
- 5- The addition of  $Y_2O_3$  has improved the dielectric properties of the ferrite.
- 6- SEM micrographs are established that the use of nanopowder produced by sol-gel technology leads to uniform and dense ferrite bodies, where the structure is compact with fewer amounts of pores.


## REFERENCES

1. J. Smit and H. P. Wijn “ ferrite, physical properties of ferromagnetic oxides in relation to their technical application’ ( Philips , Eindhoren ) . 1954
2. M.A.Dar, K.M.Batto, V. Verma, and W. Siddiui J.of alloys compounds, vol.553, 2010.
3. M.R. Bhandare, H.V.Jamadar, A.T.Pathan and A.M.Shaikh “J. of alloys compounds, vol.509, 2292-2295, 2011.
4. A. S. Boxer, F. John and D. F. Robert, “Hand book of microwave ferrite materials ”, edited by Wilhelm H. Von Aulocle,

- Academic Press New York and London, Vol.407, pp (269-271) ,1965.
5. J. Jiang, L. Li and F. Xu, “preparation and characterization of microwave ferrite materials”, edited by Wihelm H. Von Aulock, Academic by Press New York and London, Vol.407, pp(269-271), 1965.
  6. P. V. Reddy, “Charge transport in Li-Ni ferrosinels”, J. Appl. Phys, Vol. 63, No.8, pp (3783-3785),1988.
  7. G. V. M. Jacintho, A. G. Brolo, P. Corio, P. A. Z. Suarez and J. C. Rubim, “ Structural investigation of  $MFe_2O_4$  (M) Fe, Co) magnetic fluids”, J. Phys. Chem. C, Vol. 113, PP (7684–7691) , 2009.
  8. S. A. Mazen and T. A. Elmosalami, “Structural and elastic properties of Li-Ni ferrite”, Zagazig Egypt, Article ID (820726), PP (9), 2011.
  9. [M. Arana](#) [P.G. Bercoff](#) and [S. E. Jacobo](#), “Li-substituted Mn-Zn ferrite: structural and Magnetic Properties After Different Thermal Treatments”, Pro. Materials Science, Vol.1, PP(620-627), 2012.
  10. [J. Mohapatra](#), [A. Mitra](#), [D. Bahadur](#) and [M. Aslam](#), “ Surface controlled synthesis of  $MFe_2O_4$  (M = Mn, Fe, Co, Ni and Zn) nanoparticles and their magnetic characteristics”, Cryst. Eng. Comm. , Vol.15, PP (524-532), 2013.
  11. F.A.Chyad, M.S.hamza and Z.I. Dhary”Synthesis and studying dielectric properties of mixed nanoferrites”to be publish in J.of Engineering and technology, Vol. no.1, 2015.

12. C. Nlebedim and D. Jiles, "Effect of titanium substitution on the structural and magnetic properties of cobalt ferrite", Bulletin of the American Physical Society, Vol. 59, No. 1, 2014
13. W. R. Agami, M. A. Ashmawy and A. A. Sattar, "Structural, IR, and magnetic studies of annealed Li-ferrite nano-particles", J. Of Materials Engineering and Performance, Vol.23, No.2, PP (604-610), 2014.
14. F.A.Chyad, M.S.Hamza and Z.I.Dhary "Physical and mechanical properties of synthesized doped nanoferrite" to be publish in J of Engineering and technology, 2015
15. A. T. Pathan and A. M. Shaikh , "Dielectric properties of Co-substituted Li-Ni-Zn nanostructured ferrites prepared through chemical route", International J. of Computer Applications ,Vol. 45, No. 21 , PP (0975–8887), 2012.
16. A. Edelstein and R. Cammarata, "Nanomaterials synthesis, properties and applications", Chp.8, PP (1710), IOP Publishing Ltd, 1996.
17. K.R.Krishna, D.Ravindar, K.V.Kumer and C.H.Lincoln "Synthesis, XRD, SEM studies of zinc substituted in nickel ferrite. J.Of condensed Matt.Physics , Vol. 2, PP (153-159), 2012.
18. Y. P. Fu and S. H. Wu, "Electrical and magnetic properties of Mg substitution", Ceramic International, Vol. 36, PP (1311-1317), 2010.
19. J. C. Maxwell, Electricity and Magnetism, Oxford Univ. Press, Oxford, Vol. 1, Section 328, 1956.
20. A. M. Shaikh, S. S. Bellaid and B. K. Chougule, "Temperature and frequency-dependent dielectric properties of Zn substituted Li-Mg ferrites", J. Magn. Magn. Mater. Vol. 195, PP (384-390), 1999.
21. P. V. Reddy, Ph.D. Thesis, Osmania Univ., Hydrabad India, 1981.
22. R. Andrievski and A. Glezer, "Size effects in properties of nanomaterial's ", Elsevier Science Ltd., Vol. 44, PP (1621-1624), 2001.
23. B. K. Kumar, G. P. Srivastava and P. Kisher, Proc. 1CF5 (Bombay), Vol. 233, 1988.
24. M. A. Ahmed, E. Aetia, L. Salah and A. Elgamal, Materials Chemistry and Phsics., Vol. 92, PP (310-321), 2005.
25. R. V. Mangalraja, S. A. Kumar, P. Manohar and F. D. Gnanam, J. Magn. Magn. Mater. Vol. 253, PP (56), 2002.

**Author Bibliography**

	<p>Fadhil Attiya Chyad is a Professor of industrial technology at materials engineering department, University of technology, IRAQ Dr. Chyad has received his Ph.D. in industrial technology from Bradford University U.k in 1989.Dr.Chyad has an extensive research background in manufacturing, structural and synthesis aspect of materials.Dr.Chyad has published (128) scientific and technical papers in the field of ceramics, composites and powder technology. He is a supervisor of (30) PhD and MSc. Students and he is a chief and member of more than (140) examination committee. He is on editorial board for engineering and technology.</p> <p>Email: fchyad_2009@yahoo.de</p>
---	---